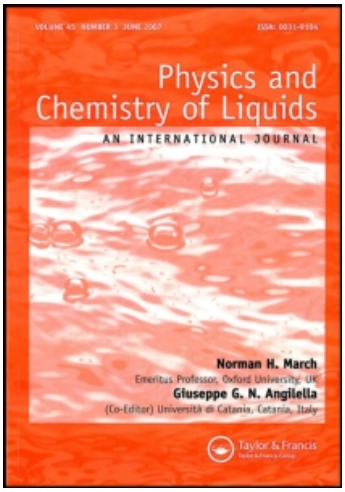

Physics and Chemistry of Liquids
Publication details, including instructions for authors and subscription information:
http://www.informaworld.com/smpp/title~content=t713646857

Phase Diagram and Rayleigh-Brillouin Scattering in Binary Solutions of Organic Compounds with Miscibility Gap

S. Kawase[a]; K. Maruyama[b]; S. Tamaki[c]; H. Okazaki[d]
[a] College of Biomedical Technology, Niigata University, Niigata, Japan [b] Graduate School of Science and Technology, Niigata University, Niigata, Japan [c] Department of Physics, Faculty of Science, Niigata University, Niigata, Japan [d] College of General Education, Niigata University, Niigata, Japan

To cite this Article Kawase, S. , Maruyama, K. , Tamaki, S. and Okazaki, H.(1994) 'Phase Diagram and Rayleigh-Brillouin Scattering in Binary Solutions of Organic Compounds with Miscibility Gap', Physics and Chemistry of Liquids, 27: 1, 49 — 63
To link to this Article: DOI: 10.1080/00319109408029508
URL: http://dx.doi.org/10.1080/00319109408029508

Phys. Chem. Liq., 1994, Vol. 27, pp. 49–63
Reprints available directly from the publisher
Photocopying permitted by license only

PHASE DIAGRAM AND RAYLEIGH-BRILLOUIN SCATTERING IN BINARY SOLUTIONS OF ORGANIC COMPOUNDS WITH MISCIBILITY GAP

S. KAWASE

College of Biomedical Technology, Niigata University, Asahimachi-dori, Niigata 951, Japan

K. MARUYAMA

Graduate School of Science and Technology, Niigata University, Igarashi, Niigata 950-21, Japan

S. TAMAKI

Department of Physics, Faculty of Science, Niigata University, Igarashi, Niigata 950-21, Japan

H. OKAZAKI

College of General Education, Niigata University, Igarashi, Niigata 950-21, Japan

(Received 7 July 1993)

The phase diagrams of binary solutions of C_6H_{14}—CH_3OH and C_6H_{12}—CH_3OH have been determined. The thermodynamic quantities of mixing, such as concentration-concentration fluctuation in the long wavelength limit, $S_{cc}(0, c, T)$, have been derived by using the treatment of Bhatia and March. The Rayleigh-Brillouin scattering has also been investigated for these solutions. $S_{cc}(0, c, T)$'s obtained by Rayleigh-Brillouin experiments were in agreement with those obtained by thermodynamical treatment of the phase diagram. The Rayleigh peak intensity of C_6H_{14}—CH_3OH system shows a weak position dependence from the interfacial boundary, in the case of the coexistence of two phases, while that of C_6H_{12}—CH_3OH does not shown such an unusual behavior. These different behaviors are discussed in terms of the densities of the components.

KEY WORDS: Rayleigh Brillouin scattering, phase diagram, miscibility gap.

1. INTRODUCTION

The light scattering from a liquid is related to Van Hove's space time correlation function in the hydrodynamic region, $S(q, \omega)$ (Van Hove 1954). As is well known, the hydrodynamic form of the van Hove correlation function is essentially given by the Rayleigh peak and the Brillouin doublet peaks in light scattering experiments.

The total integrated intensity of the Rayleigh and Brillouin peaks of $S(q, \omega)$ in the hydrodynamic region is equal to the structure factor, $S(q)$. The wavelength of visible

light is, however, much greater than the nearest neighbor interparticle spacing in liquids. Therefore, the Rayleigh-Brillouin scattering from liquids gives fully the information of the structure factor in the long wavelength limit, $S(0)$.

In a binary mixture of liquids, these discussions can be extended by Bhatia and Thornton (1970) and March *et al.* (1973).

This encourages us to carry out the determination of the phase diagram for binary liquid solutions with miscibility gaps and also to perform the experiments of the Rayleigh-Brillouin scatterings for them, in order to discuss the results by thermodynamical view-points.

In this paper, we report the phase diagrams and Rayleigh-Brillouin peak intensities for the miscibility gap systems C_6H_{14}—CH_3OH and C_6H_{12}—CH_3OH.

2. EXPERIMENTAL

2.1 Determination of phase diagram

The samples used in the present experiment were commercially available reagents with 99.9 mol.% purity and their mixtures. The sample containers were small glass cylinders with screw caps and their capacity was about 1.5 ml. For each system (C_6H_{14}—CH_3OH and C_6H_{12}—CH_3OH), 21 sample solutions were prepared with 5% step in molar concentration. The sample with container was set in a water bath, which was made of glass vessels to be transparent. Each container had a small float to keep it at the middle of the water bath. The sample container was shaken for several times during heating up or cooling down in the water bath which itself was also stirred up for all the time. After the sample solution was turned to be one phase, the temperature of the water bath was kept at a temperature higher than that of the phase transition to some extent. Then heating was stopped. We have determined the transition temperature of the solution into two phases under the cooling of the water bath at rate of 1°C/10 min. The phase separation was recognized by the beginning of sample solution being cloudy. The newly determined phase diagrams for the present systems are shown in Figures 1 and 2.

2.2 Measurements of Rayleigh-Brillouin scattering

Figure 3 shows a block diagram of the measuring system of the Rayleigh and the Brillouin scattering intensity. The instrument is combined by a single-mode argon-ion laser (NEC, GLG3460), a Fabry-Perot interferometer (MIZOJIRI, FP-T30), a lock-in amplifier (NF, LI-570A), and an X-Y recorder (RIKEN DENSHI, F-5C). The exciting light wavelength was 514.5 nm and the laser power was about 500 mW. The light beam was chopped at 225 Hz and focused at the center of a sample cell by a lens L_1 (focal length $f_1 = 3$ cm). The size of sample glass cell was 12ϕ (outer diameter) $\times$ 32 mm (height) with a screw cap. The light scattered to a right angle was focused by a lens L_2 (focal length $f_2 = 25$ cm) onto a slit (slit width 0.5 mm) of a monochromator. The light passing through the monochromator was made being parallel by a lens L_3 (focal length $f_3 = 20$ cm), and analysed by the Fabry-Perot interferometer. The spacer between the

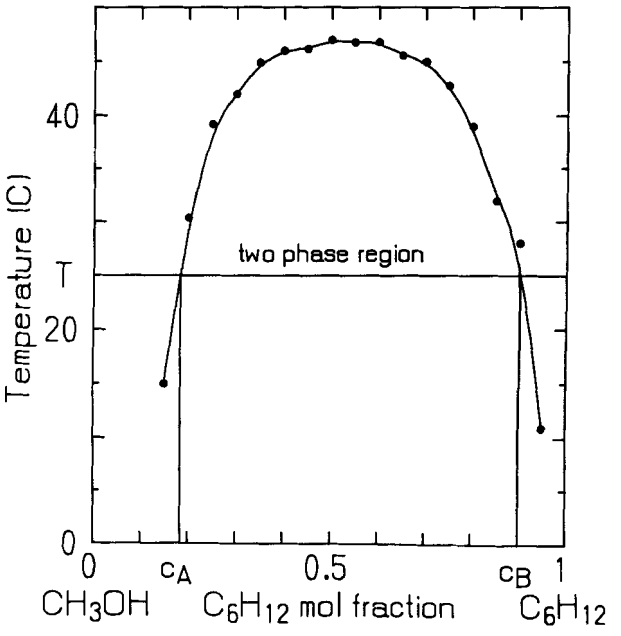

Figure 1 The phase diagram of CH_3OH — C_6H_{12} system.

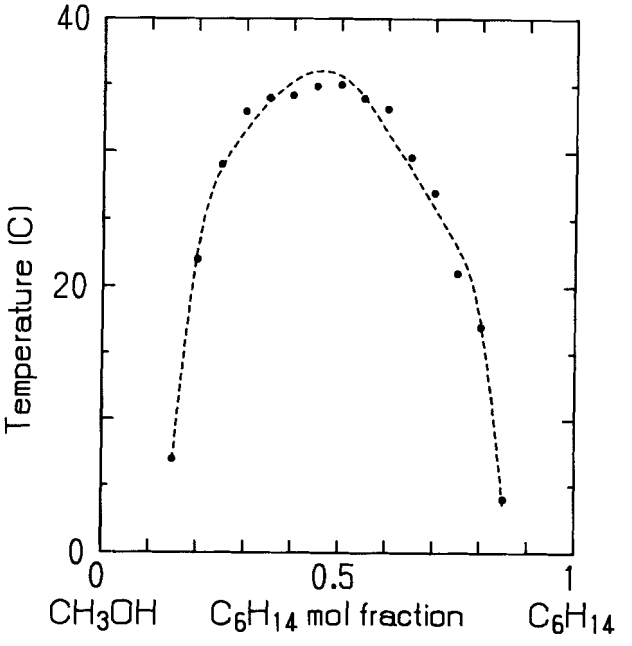

Figure 2 The phase diagram of CH_3OH — C_6H_{14} system. The broken line shows calculated values from Figure 7 and Eq. (4).

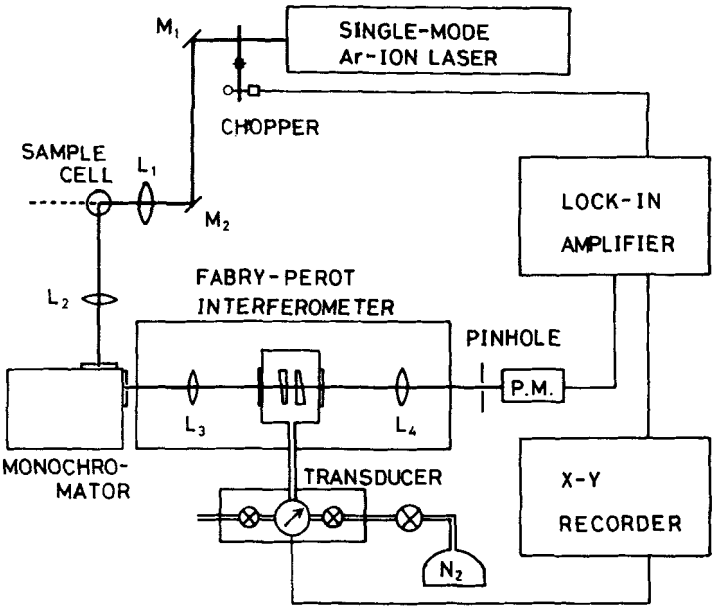

Figure 3 A block diagram of the measuring system of the Rayleigh and Brillouin scattering. M_1 and M_2: mirrors; L_1, L_2, L_3 and L_4: lenses; ⊗: valves.

interferometer etalons has a thickness of 6.030 mm, giving a free spectral range of 0.829 cm^{-1}, and an overall instrumental half-width of about 0.015 cm^{-1}, varying slightly for different alignments. The interferometer was pressure-scanned by supplying nitrogen gas to the chamber enclosing the etalons. The interferometer output was focused onto a screen by a lens L_4 (focal length $f_4 = 30$ cm). The light passing through a pinhole (diameter = 0.3 mm) on the screen was detected by a photomultiplier tube (HAMAMATSU PHOTONICS, R647-04). The output current from the tube was led into the lock-in amplifier. The time constant of the lock-in amplifier was chosen as 0.3s which was found to be sufficient for S/N ratio. The reference signal to the lock-in amplifier was synchronized with the light chopper. The output of the lock-in amplifier was indicated on the X-Y recorder. The X-axis of the recorder was supplied from the transducer of pressure of the interferometer to the voltage. The scattering spectrum is also stored in a microcomputer, and some parameters, such as intensities and Brillouin shifts, are obtained by using least square fitting method.

The samples used in this experiment were made dust-free by using a membrane filter (ADVANTEC, DISMIC) with a pore size of 0.2 μm. The test of a solution being dust-free was done by comparing the observed Rayleigh intensity with the true Rayleigh intensity of dust-free samples. We see that mixture samples can be dust-free by the same method as that applied for pure liquids. The observed light scattering spectra for the present systems are shown in Figures 4 and 5.

The sample temperature was kept at 25°C within the accuracy of 0.5°C during the course of measurements.

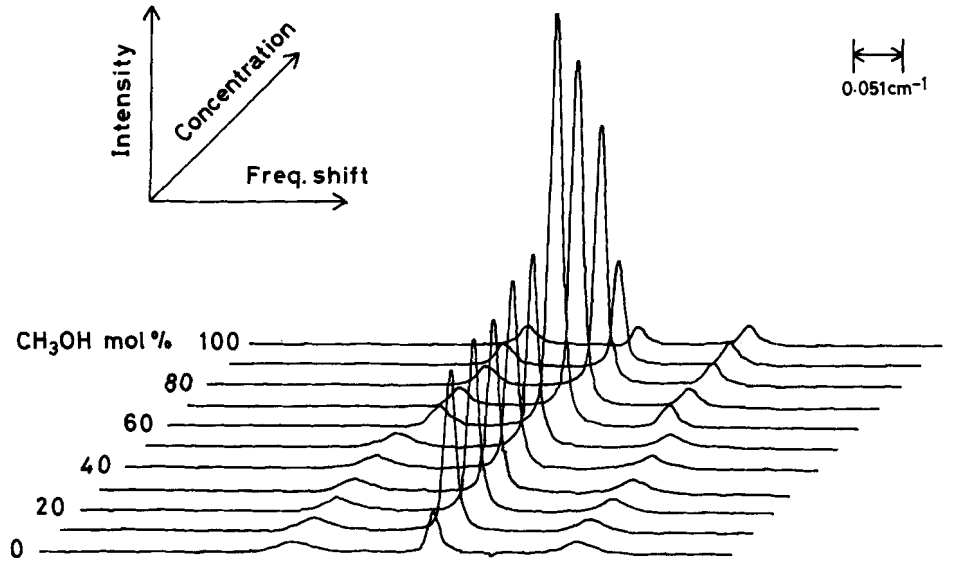

Figure 4 The observed light scattering spectra of CH_3OH — C_6H_{12} mixtures and their variation with the composition change. The horizontal bars in the both sides of spectrum represent the base line. The molar fraction of C_6H_{12} is indicated in the figure.

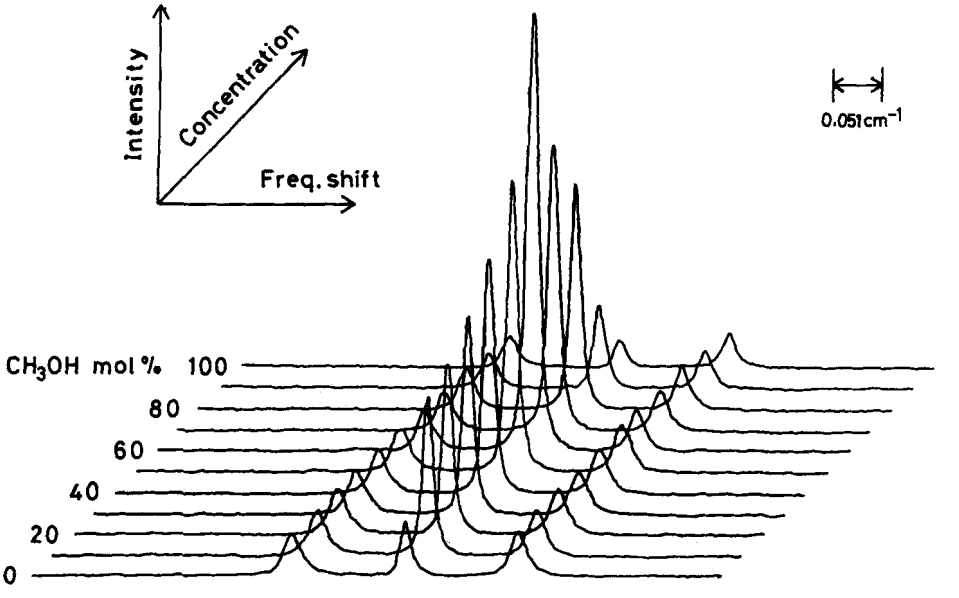

Figure 5 The observed light scattering spectra of CH_3OH — C_6H_{14} mixtures and their variation with the composition change. The horizontal bars in the both sides of spectrum represent the base line. The molar fraction of C_6H_{14} is indicated in the figure.

3. THERMODYNAMICS OF PHASE DIAGRAM

The present systems exhibit a two-phase region and consequently they are not described by a conformal solution theory. However the solution in the one phase of their systems may be analyzed in terms of a modified conformal solution (MCS) theory (Flory, 1942) which includes the effect of size difference of the constituents.

The Gibbs free energy for a binary solution $A_{c_A}B_{1-c_A}$ by MCS theory is given by the following form (Tamaki, 1987),

$$G = c_A G_A^0 + (1-c_A)G_B^0 + Nk_BT\{c_A \ln\phi + (1-c_A)\ln(1-\phi)\} + Nc_A(1-c_A)g(c_A)w, \quad (1)$$

where G_i^0 is Gibbs free energy of the i constituent in its pure state and $g(c)$ is a function of the concentration and is assumed to be expressed by a polynomial $g(c) = 1 + Ac + Bc^2 + Cc^3 + Dc^4 + Ec^5 + Fc^6$.

The concentration-concentration fluctuation in the long wavelength limit, $S_{cc}(0, c, T)$, defined by Bhatia-Thornton (B-T) is, then, equal to

$$S_{cc}(0,c,T) = Nk_BT \Big/ \left(\frac{\partial^2 G}{\partial c_A^2}\right)_{N,p,T} = c_A(1-c_A)\left[1 + c_A(1-c_A)\delta^2 + c_A(1-c_A)g''(c_A)w/k_BT\right]^{-1}, \quad (2)$$

where

$$\delta = \frac{1}{V}\left(\frac{\partial V}{\partial c_A}\right)_{N,p,T}. \quad (3)$$

From the coexistence curve for two phases, the interaction function $g''(c_A)w$ is derived by using least square fitting with the following condition

$$\left[1 + c_A(1-c_A)\delta^2 + c_A(1-c_A)\,g''(c_A)w/k_BT\right] = 0. \quad (4)$$

Figures 6 and 7 show $g''(c)w/k_B$ derived from the experimental data of the phase diagram, the experimental densities (Joerges and Nikuradse 1950, and Harms 1942/43) and equation (4) (closed circles), and least square fitted curve with a fourth order polynomial of $g''(c_A)w$. As seen in these figures, agreement is very good. Reversely using this $g''(c_A)w$, the phase separation temperature can be estimated with an error smaller than a few degrees (broken line in Figure 2). If the system is completely described in terms of an ideal regular solution model, Eq. (4) is converted to

$$1 - \frac{2c_A(1-c_A)w}{k_BT} = 0. \quad (5)$$

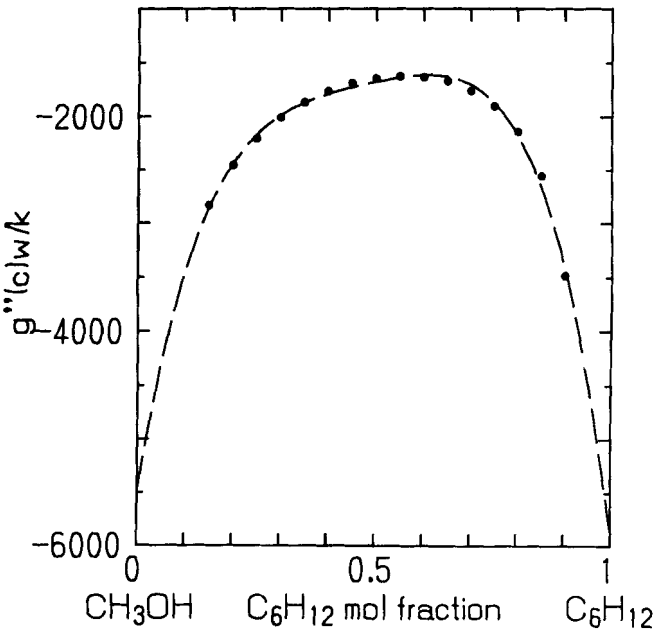

Figure 6 The interaction parameter $g''(c)w$ for $CH_3OH - C_6H_{12}$ system as a function of concentration. The closed circles are derived from phase diagram and broken line is a result of least square fitting with a fourth order polynomial.

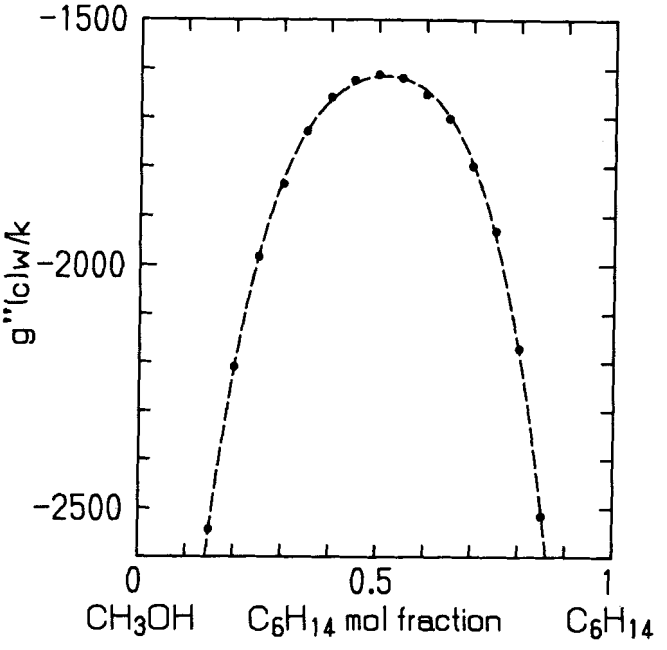

Figure 7 The interaction parameter $g''(c)w$ for $CH_3OH - C_6H_{14}$ system as a function of concentration. The closed circles are derived from phase diagram and broken line is a result of least square fitting with a fourth order polynomial.

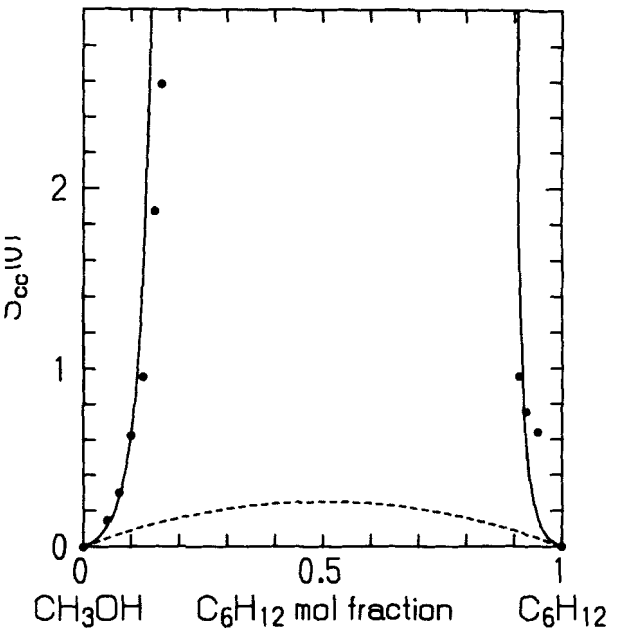

Figure 8 $S_{cc}(0)$ for $CH_3OH - C_6H_{12}$ system as a function of concentration at 25°C. Solid line is obtained from fitted $g''(c)w$ and Eq. (2), and closed circle is derived from light scattering intensities and Eq. (11). Broken line represents the $S_{cc}(0)$ for ideal mixture.

From $g''(c)$ we can calculate $S_{cc}(0)$ for one phase region by Eq. (2). Figures 8 and 9 show calculated $S_{cc}(0)$ by solid lines for $CH_3OH - C_6H_{12}$ and $CH_3OH - C_6H_{14}$ systems, respectively. Furthermore by using $S_{cc}(0)$ and the condition $g(0) = g(1) = 1$ which may correspond to the Henry's law in the activity coefficient, we can estimate the quantities, $\Delta G(\equiv G - c_A G_A^0 - (1 - c_A)G_B^0)$ and thereafter $g(c_A)$ and w. Calculated values of ΔG, $g(c_A)$ and w are shown in Figures 10 and 11, and Table 1, respectively.

4. THEORETICAL BACKGROUND OF RAYLEIGH-BRILLOUIN SCATTERING

By analogy with Van Hove's neutron scattering formalism (Van Hove 1954), and Komarov and Fisher (1963), the intensity $I(R, \omega)$ of light scattered from fluid, per unit incident intensity, per unit solid angle, per unit frequency range ω, is given by the following expression

$$I(R, \omega) = \left(\frac{N\alpha_e^2\Omega_0^4}{2\pi R^2 c^4}\right) \sin^2\varphi \, S(q, \omega), \tag{6}$$

where N is the number of molecules in the fluid, α_e an effective polarization per molecule, Ω_0 the angular frequency of incident light, ω the angular frequency difference

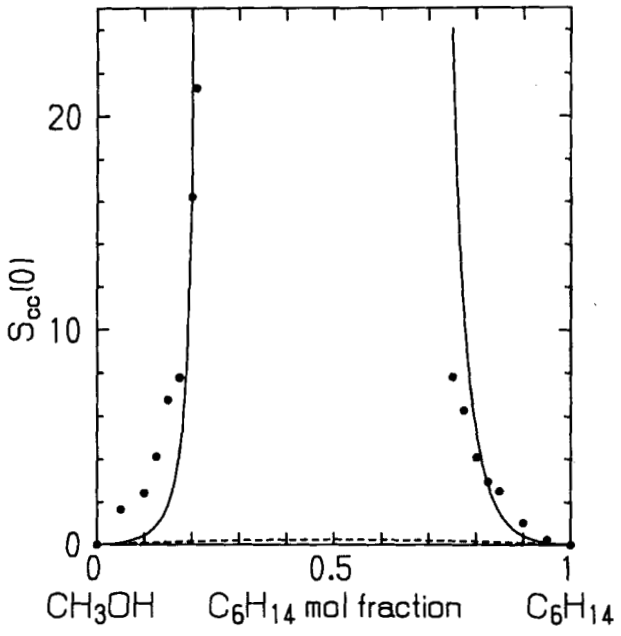

Figure 9 $S_{cc}(0)$ for CH_3OH — C_6H_{14} system as a function of concentration at 25°C. Solid line is obtained from fitted $g''(c)w$ and Eq. (2), and closed circle is derived from light scattering intensities and Eq. (11). Broken line represents the $S_{cc}(0)$ for ideal mixture.

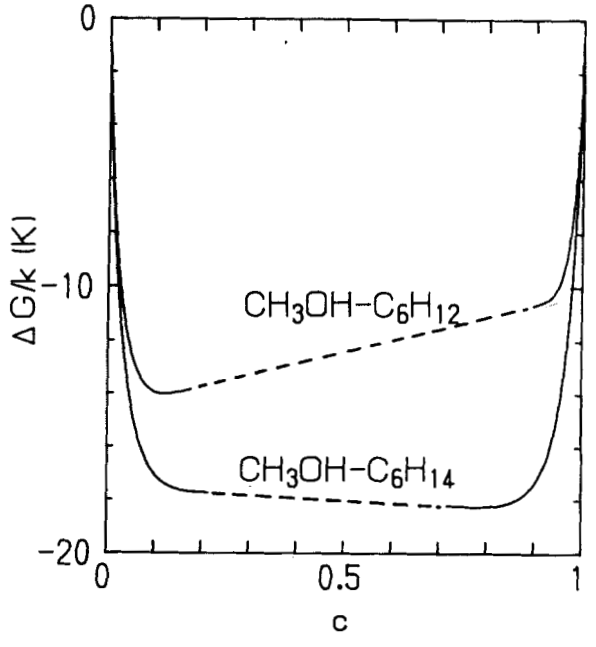

Figure 10 Calculated ΔG for CH_3OH — C_6H_{12} and CH_3OH — C_6H_{14} systems. Broken lines represent the two phase region.

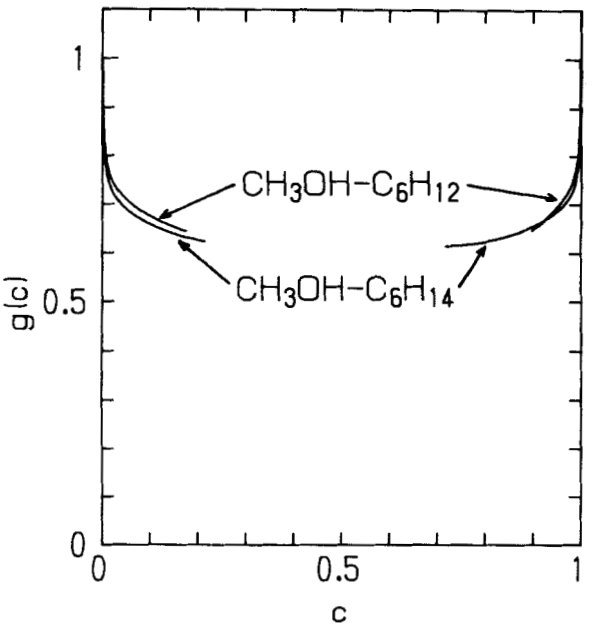

Figure 11 Obtained $g(c)$ from Figure 10 for $CH_3OH - C_6H_{12}$ and $CH_3OH - C_6H_{14}$ systems.

Table 1 Interaction parameter ω calculated from Eq. (1).

system	$\omega/k(K)$
$CH_3OH - C_6H_{12}$	1533.5
$CH_3OH - C_6H_{14}$	1466.9

of the incident and scattered lights, c the velocity of light in vacuum, R the distance from the scattered center, φ the angle between the direction observation and the direction of electric vector in the incident light, and $S(q, \omega)$ the space and time Fourier transform of the two-body correlation function $G(r, t)$ which is defined by Van Hove, q being the wave vector corresponding to ω.

The observed integrated intensity $\mathscr{I}$ corresponds to

$$\mathscr{I} = \mathscr{I}_R + 2\mathscr{I}_B = K \int I(R, \omega)\, d\omega, \tag{7}$$

where K is a constant determined by the condition of measurements. Equation (7) is converted to (Bhatia and Tong, 1968)

$$\mathscr{I} = K'S(q) = K'(c_A^2 a_{AA}(q) + 2c_A c_B a_{AB}(q) + c_B^2 a_{BB}(q)), \tag{8}$$

where $K' = K(N\alpha_e^2\Omega_0^4/2\pi R^2 c^4)\sin^2\varphi$ and the a_{ij} are the so-called Faber-Ziman

structure factors (Faber and Ziman, 1965) expressed as

$$a_{ij}(q) = 1 + \int_0^\infty 4\pi r^2 \rho [g_{ij}(r) - 1] \frac{\sin(qr)}{qr} dr, \tag{9}$$

where ρ is the number density and g_{ij}'s are the partial pair distribution functions.

Since the wavelength of the incident beam of light is the order of 5000Å and is very large compared to the correlation length between molecules, we can discuss the Rayleigh scattering results by $a_{ij}(q)$ in the long wave length limit as $q \to 0$. According to B-T, $a_{ij}(0)$'s (i, j = A, B) for a binary fluid mixture A–B are given by March and Tosi (1976)

$$\begin{aligned} a_{AA}(0) &= \frac{Nk_BT}{V_M}\chi_T - \frac{c_B}{c_A} + S_{cc}(0, c_A, T)\left(\delta - \frac{1}{c_A}\right)^2, \\ a_{BB}(0) &= \frac{Nk_BT}{V_M}\chi_T - \frac{c_A}{c_B} + S_{cc}(0, c_A, T)\left(\delta + \frac{1}{c_B}\right)^2, \\ a_{AB}(0) &= \frac{Nk_BT}{V_M}\chi_T + 1 + S_{cc}(0, c_A, T)\left(\delta - \frac{1}{c_A}\right)\left(\delta + \frac{1}{c_B}\right), \end{aligned} \tag{10}$$

where χ_T the isothermal compressibility. Combining Eqs. (9) and (10), we obtain the scattering intensity $\mathscr{I}$ as

$$\mathscr{I} = K'\left[\frac{Nk_BT}{V_M}\chi_T + S_{cc}(0, c, T)\delta^2\right]. \tag{11}$$

So far the integrated scattering intensity is fully expressed in terms of the three thermodynamic quantities, χ_T, $S_{cc}(0)$ and δ except for the experimental constant K'. The constant K' in this expression can be experimentally obtained so as to fit the observed intensity $\mathscr{I}$ of pure component by using the isothermal compressibility χ_T which is numerically close to 1.1 χ_s.

The adiabatic compressibility χ_s is given by

$$\chi_s = \frac{1}{\rho v_s^2}, \tag{12}$$

where v_s is the sound velocity of liquid and is related to the Brillouin shift. In the following section, we will analyze our experimental results for the Rayleigh-Brillouin scattering by using the above formulae.

5. $S_{cc}(0, c, T)$ OBTAINED FROM RAYLEIGH-BRILLOUIN SCATTERING

Comparing Eq. (11) and the experimental data of Rayleigh-Brillouin scattering intensities, we have obtained $S_{cc}(0, c, T)$ for the one-phase solutions at the room temperature, under the assumption that $\chi_T = 1.1\chi_s$ and $\chi_s \simeq (c_A V_A/V)\chi_s^A + (1 - c_A)V_B/V\chi_s^B$. $S_{cc}(0, c, T)$ obtained for the present systems are shown in Figures 8

and 9. They agreed quantitatively with those obtained by analyzing the coexistence curves of two phases with the help of modified conformal solution theory.

6. ANOMALOUS BEHAVIOR IN THE RAYLEIGH SCATTERING FOR C_6H_{14} — CH_3OH SYSTEM

As described in the above, the present system have a two-phase separation. CH_3OH — C_6H_{12} system has a fairly small difference in the densities and indicates a

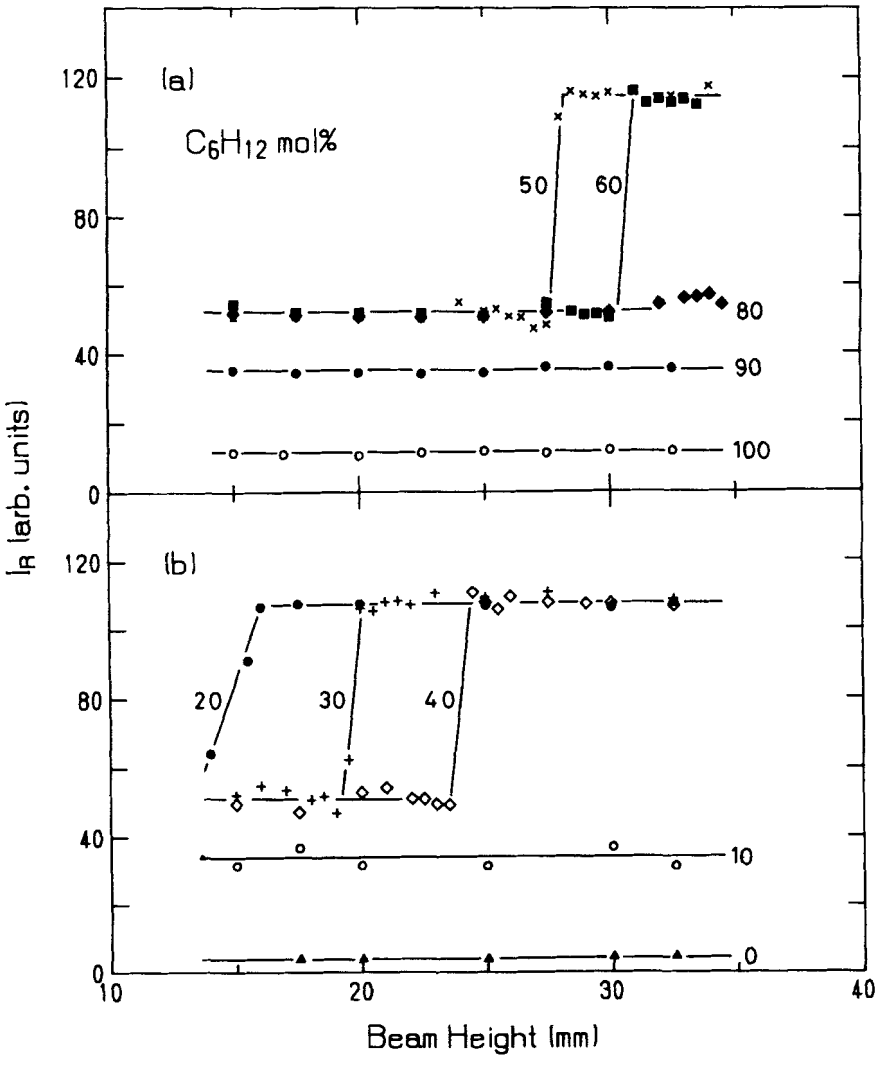

Figure 12 The observed Rayleigh scattering intensity for CH_3OH — C_6H_{12} system as a function of a light beam position. The molar fraction of C_6H_{12} is indicated in the figure. The curves in the figure are guides for the eyes.

miscibility gap of two phases at room temperature. In the procedure of making a sample, if their concentration ratio is given as c, even after shaking fully the container, the sample may be divided into two phases as A and B as seen in Figures 1 and 2. So the down-side fluid must be A and the up-side one is B.

In the fluid A, the C_6H_{12} of c_A mol% is dissolved into CH_3OH. In a similar way CH_3OH of $1-c_B$ mol%is dissolved into C_6H_{12} in the fluid B. Therefore, all samples with the nominal concentration ratio at c, if it is in the range between c_A and c_B at a given temperature T as seen in Figures 1 and 2, should be separated into the two phases as A and B by the amount of $(c_B - c)$ and $(c - c_A)$.

The scattering intensities have been measured for various position of the specimen container (Figure 12). The top and the bottom of the container correspond to 15mm and 35mm of beam height in Figure 12, respectively. Step-wise intensities are caused by the crossing the up-side phase to the down-side one. These have no height dependence and the concentration dependencies are shown in Figure 13.

In a similar way to the case of C_6H_{12} — CH_3OH system, the samples were prepared and then the Rayleigh scatterings were measured. The scattering intensities as a function of the depth from the top of the fluids were shown in Figure 14.

From 30 to 70 mol% C_6H_{14}, they form the two phase regions as seen by a kind of step-wise change. However, it is very interesting that these intensities have a position dependence. This phenomenon seems to be quite unusual. As far as seen in the $c - T$

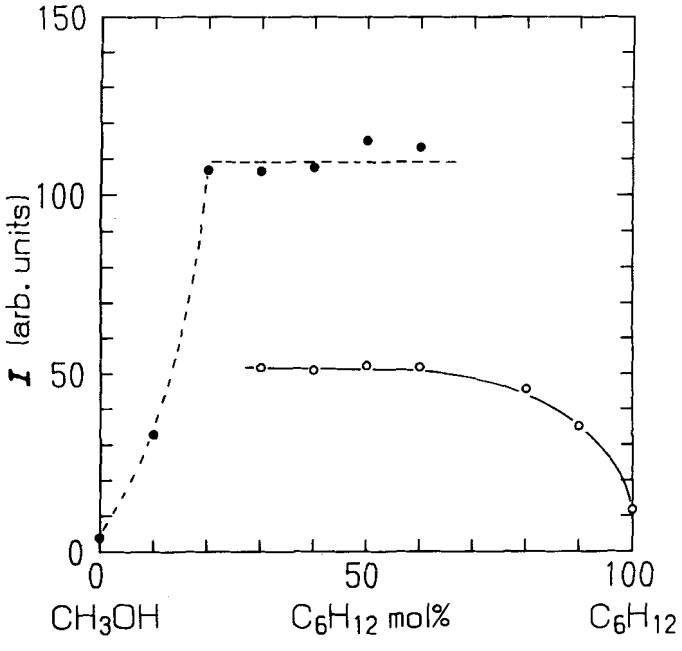

Figure 13 The Rayleigh scattering intensity near the phase interface for CH_3OH — C_6H_{12} system as a function of the C_6H_{12} concentration. The circles and triangles represent the scattering intensities in C_6H_{12} and CH_3OH rich phases, respectively. The solid and broken curves in the figure are guides for the eyes.

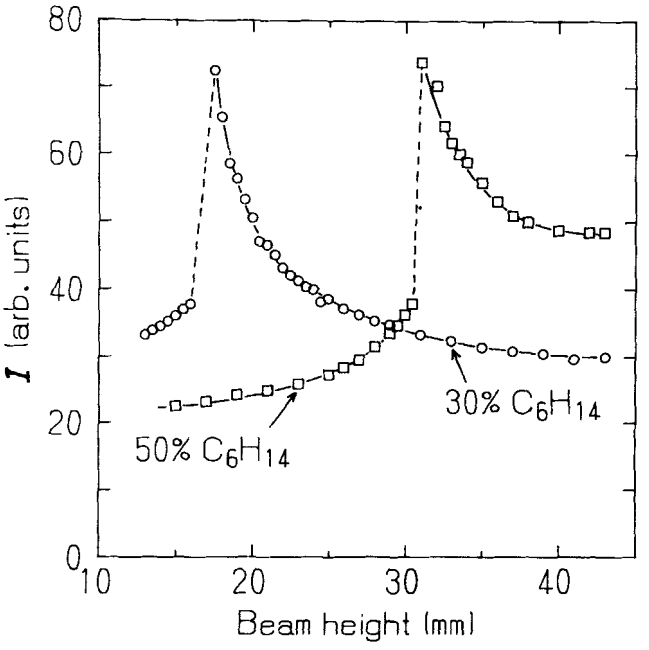

Figure 14 The observed Rayleigh scattering intensity for CH_3OH — C_6H_{14} system as a function of a light beam position. The molar fraction of C_6H_{14} is indicated in the figure. The curves in the figure are guides for the eyes.

phase diagram, both C_6H_{12} — CH_3OH and C_6H_{14} — CH_3OH mixtures show a similar feature. The difference for both mixtures is only the density of the constituents (CH_3OH:0.7914g/cm^3, C_6H_{12}:0.7763g/cm^3 and C_6H_{14}:0.6594g/cm^3). For C_6H_{12} — CH_3OH mixtures, the densities of the constituents are nearly the same, while for C_6H_{14} — CH_3OH ones, they are quite different.

In order to see whether these facts are related or not to the gravitational effect, we tried to measure the various size of containers in which the thickness of the up and down side solutions and found that the position dependence from the interfacial boundary is unique. This infers that the anomaly is not related to an explicit gravitational effect.

However, since the $S_{cc}(0, c, T)$'s at c_A and/or c_B are quite large, it may be possible to form a fine change in the pair distribution function $g_{ij}(r)$ at the position near the interfacial boundary if the densities of the constituents are quite different. Such a position dependence in the physical quantities near the interfacial boundary can be seen, for example, although their position dependence can be seen only in the length of several hundred times of the segment of liquid crystal (Ondris-Crawfold *et al.*, 1993).

At the present stage, we can not clearly answer to the question for such a macroscopic position dependence. However it may be worth while to report such a very unusual behavior.

Acknowledgements

The authors are grateful to Prof. M. Misawa for valuable discussion.

References

1. A. B. Bhatia and D. E. Thornton, *Phys. Rev. B*, **2**, 3004 (1970).
2. A. B. Bhatia and E. Tong, *Phys. Rev.*, **173**, 231 (1968).
3. T. E. Faber and J. M. Ziman, *Phil. Mag.*, **11**, 153 (1965).
4. P. J. Flory, *J. Chem. Phys.*, **10**, 51 (1942).
5. H. Harms, *Z. Physik. Chem. B*, **53**, 280 (1942/43).
6. M. Joerges and A. Nikuradse, *Z. Naturforsch.*, **5a**, 259 (1950).
7. L. I. Komarov and I. Z. Fisher, *Soviet Phys. JETP*, **16**, 1358 (1968).
8. N. H. March and M. P. Tosi, *Atomic Dynamics in Liquids* (Macmillan Press, London) (1976).
9. N. H. March, M. P. Tosi and A. B. Bhatia, *J. Phys. C*, **6**, L59 (1973).
10. R. J. Ondris-Crawfold, G. P. Crawfold, S. Žumer and J. W. Doane, *Phys. Rev. Lett.*, **70**, 194 (1993).
11. S. Tamaki, Can. *J. Phys.*, **65**, 286 (1987).
12. L. Van Hove, *Phys. Rev.*, **95**, 249 (1954).